Synthesis and Vesicle Formation from Hybrid Bolaphile/Amphiphile Ion-Pairs. Evidence of Membrane Property Modulation by Molecular Design

Santanu Bhattacharya,*,† Soma De, and M. Subramanian

Department of Organic Chemistry, Indian Institute of Science, Bangalore 560 012, India

Received February 19, 1998

Four new hybrid (bolaphile/amphiphile) ion-pairs were synthesized. Electron microscopy indicated that each of these forms bilayer membranes upon dispersion in aqueous media. Membrane properties have also been examined by differential scanning calorimetry, microcalorimetry, temperature-dependent fluorescence anisotropy measurements, and UV−vis spectroscopy. The T_m values for the vesicular **1**, **2**, **3**, **4**, and **5** were 38, 12, 85, 31.3, and 41.6 °C, respectively. Interestingly the T_m values for **1** and **3** were found to depend on their concentration. The entrapment of small solute and the release capability have also been examined to demonstrate that these bilayers form enclosed vesicles. X-ray diffraction of the cast films has been performed to understand the nature and the thickness of these membrane organizations. The membrane widths ranged from 33 to 47 Å. Finally, the above observations have been analyzed in light of the results obtained from molecular modeling studies. Thus we have demonstrated that membrane properties can be modulated by simple structural changes at the amphiphile level. It was shown that by judicious incorporation of central, isomeric, disubstituted aromatic units as structural anchors into different bolaphiles, one can modulate the properties of the resulting vesicles.

Introduction

Lipids and related amphiphiles are important building blocks of biological membranes.[1] Several naturally occurring lipids have been isolated from sources as diverse as plants, mammalian tissues, bacteria and even marine organisms.[2−5] However, due to the extreme difficulties associated with their isolation, effective purification, and characterization, most of the biophysical approaches to understanding membrane behavior at the molecular level have been largely devoted to synthetic analogues of lipids. In addition, synthetic amphiphiles that form micellar or vesicular aggregates in aqueous media are also attractive for their potential applications in drug delivery,[6] catalysis,[7] and the synthesis of nanomaterials.[8] Consequently, attempts to correlate the physical properties of membranes from a structurally defined lipid or its analogues are currently receiving widespread interest. Early pioneering studies in this direction demonstrated the feasibility of exploring various membrane-forming properties from molecules of totally synthetic, nonbiological origin.[9] Since then, investigations by different research groups[10] including ourselves[11] on synthetic lipids and amphiphiles have enriched the understanding in this area considerably.

It is known that by mixing single chain amphiphiles of same charge in water, one can obtain mixed micelles.[12] However, when equivalent amounts of single chain amphiphiles of opposite charges are mixed, lamellar or bilayer type aggregates are produced.[13] Presumably the electrostatic interactions at or near the headgroup region

† Fax: 91-080-334-1683. E-mail: sb@orgchem.iisc.ernet.in. Also at the Chemical Biology Unit, Jawaharlal Nehru Centre for Advanced Scientific Research, Jakkur, Bangalore 560 064, India.

(1) (a) Merz, K. M., Jr.; Roux, B. *Biological Membranes. A Molecular Perspective from Computation and Experiment*; Birkhäuser, Boston, 1996. (b) Slater, J. L.; Huang, C.-H. In *The Structure of Biological Membranes*; Yeagle, P., Ed.; CRC Press: Boca Raton, FL, 1992; pp 175−210. (c) Marsh, D. *CRC Handbook of Lipid Bilayers*; CRC Press: Boca Raton, FL, 1990.

(2) (a) Grunner, S. M.; Jain, M. K. *Biochim. Biophys. Acta* **1985**, *818*, 352. (b) Bittman, R.; Clejan, S.; Jain, M. K.; Deroo, P. W.; Rosenthal, A. F. *Biochemistry* **1981**, *20*, 2790. (c) Friedberg, S. J.; Holpert, M. *J. Lipid. Res.* **1978**, *19*, 57.

(3) Langworthy, T. A. In *The Bacteria. The Treatise on Structure and Function*; Woese, C. R., Wolfe, R. S., Eds.; Academic: Orlando, FL, 1985; pp 459−497. De Rosa, M.; Gambacorta, A.; Gliozzi, A. *Microbiol. Rev.* **1986**, *50*, 70.

(4) Setter, K. O. *Nature* **1982**, *300*, 258.

(5) Brock, T. D.; Brock, K. M.; Belley, R. T.; Weiss, R. L. *Arch. Mikrobiol.* **1972**, *84*, 54.

(6) Ringsdorf, H.; Schlarb, B.; Venzmer, J. *Angew. Chem., Int. Ed. Engl.* **1988**, *27*, 113.

(7) (a) Bhattacharya, S.; Snehalatha, K.; George, S. K. *J. Org. Chem.* **1998**, *63*, 27. (b) Bhattacharya, S.; Snehalatha, K. *Langmuir* **1995**, *11*, 4653. (c) Scrimin, P.; Tecilla, P.; Tonellato, U. *J. Am. Chem. Soc.* **1992**, *114*, 5086.

(8) (a) Schnur, J. M. *Science* **1993**, *262*, 1669. (b) Whitesides, G. M.; Mathias, J. P.; Seto, C. T. *Science* **1991**, *254*, 1312.

(9) (a) Kunitake, T. *Angew. Chem., Int. Ed. Engl.* **1992**, *31*, 2137. (b) Fendler, J. H. *Science* **1984**, *223*, 888. (c) Fendler, J. H. *Membrane Mimetic Chemistry*; Wiley: New York, 1982.

(10) (a) Sommerdijk, N. A. J. M.; Hoeks, T. H. L.; Synak, M.; Feiters, M. C.; Nolte, R. J. M.; Zwanenburg, B. *J. Am. Chem. Soc.* **1997**, *119*, 4338. (b) Menger, F. M.; Ding, J. *Angew. Chem., Int. Ed. Engl.* **1996**, *35*, 2137. (c) Song, X.; Perlstein, J.; Whitten, D. G. *J. Am. Chem. Soc.* **1995**, *117*, 7816. (d) Murillo, O.; Watanabe, S.; Nakano, A.; Gokel, G. W. *J. Am. Chem. Soc.* **1995**, *117*, 7665. (e) Lee, Y.-S.; Yang, J.; Sisson, T. M.; Frankel, D. A.; Gleeson, J. T.; Aksay, E.; Keller, S. L.; Gruner, S. M.; O'Brien, D. F. *J. Am. Chem. Soc.* **1995**, *117*, 5573. (f) Moss, R. A.; Li, G.; Li, J.-M. *J. Am. Chem. Soc.* **1994**, *116*, 805. (g) Thompson, D. H.; Wong, K. F.; Humphry-Baker, R.; Wheeler, J. J.; Kim, J.-M.; Rananavare, S. B. *J. Am. Chem. Soc.* **1992**, *114*, 9035. (h) Wagenaar, A.; Rupert, L. A. M.; Engberts, J. B. F. N.; Hoekstra, D. *J. Org. Chem.* **1989**, *54*, 2638.

(11) (a) Bhattacharya, S.; Snehalatha, K. *J. Org. Chem.* **1997**, *62*, 2198. (b) Bhattacharya, S.; De, S.; George, S. K. *Chem. Commun.* **1997**, 2287. (c) Bhattacharya, S.; Mandal, S. S. *Biochim. Biophys. Acta (Biomembranes)* **1997**, *1323*, 29. (d) Bhattacharya, S.; Haldar, S. *Biochim. Biophys. Acta (Biomembranes)* **1996**, *1283*, 21. (e) Ghosh, S.; Easwaran, K. R. K.; Bhattacharya, S. *Tetrahedron Lett.* **1996**, *37*, 5769. (f) Bhattacharya, S.; Haldar, S. *Langmuir* **1995**, *11*, 4748. (g) Bhattacharya, S.; Subramanian, M.; Hiremath, U. *Chem. Phys. Lipids* **1995**, *78*, 177. (h) Bhattacharya, S.; De, S. *J. Chem. Soc., Chem. Commun.* **1995**, 651.

(12) Tanford, C. *The Hydrophobic Effect: Formation of Micelles and Biological Membranes*; Wiley: New York, 1980.

10.1021/jo980315l CCC: $15.00
Published on Web 10/03/1998

and hydrophobic association of the nonpolar chains drive the formation of "tight" complexes which eventually develop into lamellae or bilayers. However, so far these studies have been confined to amphiphilic surfactants only and the corresponding mixtures of *monopolar* amphiphile and *bipolar* bolaphiles[14] have not been examined for vesicle formation. Synthetic bolaphiles are mimics of archaebacterial membranes which can sustain extreme physiological conditions (85 °C, high pH) and form ultrathin "monolayer" membranes.[15] Due to these exceptional properties, much interest is growing toward the development of their mimics to sort out their unusual tolerance to external stimuli compared to the membrane present in other organisms. We thought that it would be interesting in this context to examine ion-pairs from a mixture of oppositely charged amphiphilic and bolaphilic molecules.

In a preliminary communication,[16] we have demonstrated that one can generate vesicles via ion-pairing of cationic amphiphile with bisanionic bolaphiles. In this paper we present in detail, the synthesis, the vesicle formation, the thermotropic behavior, and the micropolarity of a series of bis(hexadecyltrimethylammonium)-phenyl-1,2-, 1,3-, and 1,4-di(oxyundecanoate) amphiphiles **1**−**3** in which the alkyl chains of the bolaamphiphilic counterions originate from the different isomeric positions of the central phenyl ring. We also present the dye entrapment abilities of these vesicles and the results of the permeability experiments with these vesicles. Cast film X-ray diffraction studies on the multilayers were also performed to investigate the possible nature of the bilayer organization in these membranes. To put our results into proper perspective, we also examined the vesicular properties of the corresponding amphiphile (monopolar) anion/cation pair cetyltrimethylammonium (CTA) 11-phenoxyundecanoate **4** and CTA palmitate, **5**. It is evident that by judicious incorporation of central, isomeric, disubstituted aromatic units as structural anchors into different bolaphiles one can modulate the properties of the resulting vesicles. Remarkably the phase transition temperatures and the permeabilities of these vesicular aggregates were found to be highly influenced by the geometry of the bolaamphiphilic counterion. Finally, we provide a rationale for the effects of such shape variation of the bolaform counterion by considering energy-minimized structures obtained by molecular modeling studies for each amphiphile.

Results and Discussion

Molecular Design and Synthesis. To realize bilayer like assemblies from the hybrid ion-paired bolaphile/amphiphiles and to explore whether subtle structural differences in the starting ion-pairs are reflected in the properties of bilayer assemblies, we synthesized five systems, as shown in Scheme 1. Three of these compounds are composed of the following molecular modules. First, the bolaphilic counterparts in these ion-pairs contain central aromatic units from which two lipophilic chains are connected and the ends of these chains contain carboxylate residues. Second, the central aromatic units are isomeric in relation so that disubstituted (1,2-, 1,3-, 1,4-) aromatic units can act as structural anchors in these bolaphiles. Thus, depending on the position of the covalent linkage of the undecanoate chains to the central aromatic core, these lipophilic chains propagate at directions dictated by the manner in which they are connected with the respective aromatic ring. Third, the end CO_2^- residues are finally ion-paired with amphiphilic cetyltrimethylammonium (CTA^+) cations.

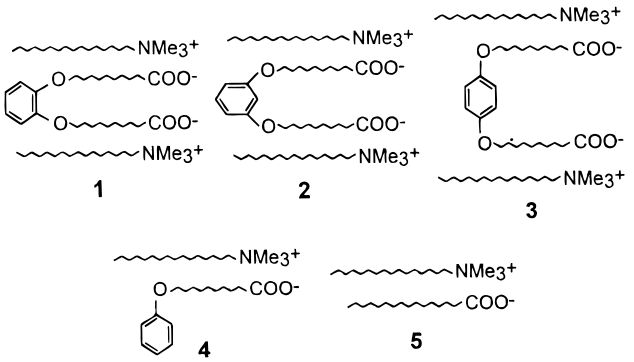

The synthesis of the ion-paired systems **1**−**4** began with the preparation of three new aromatic diacids (**8a**, **8b**, and **8c**) and one phenoxy acid (**8d**) (Scheme 1). These were accomplished by the conversion of catechol, resorcinol, quinol, and phenol to the corresponding ethers upon treatment with ethyl 11-bromoundecanoate or the corresponding acids generally in high yields. The corresponding esters were hydrolyzed in the presence of ethanolic KOH. Then the ion-paired systems (**1**−**4**) were synthesized in a key step as described below. First, by the passage of a methanolic solution of freshly recrystallized cetyltrimethylammonium bromide (CTAB) (1 equiv) through ion-exchange resin (Amberlite IRA-900, OH^- form), CTA^+OH^- was generated. Then for the preparation of **1**−**3**, to each of the reaction mixtures containing 1 equiv of CTA^+OH^-, 0.5 equiv of diacid **8a**, **8b**, or **8c**, respectively, in dry methanol was added. The reaction mixtures were stirred at room temperature for 24 h under nitrogen inlet, and the solvents were removed by rotary evaporation to obtain solid residues from each of the reaction mixtures. For the synthesis of **4**, similar reaction conditions were employed using 1 equiv of monoacid **8d** in methanol. All the compounds isolated as solids after evaporation of methanol were recrystallized several times from EtOAc/MeOH (10:1), and each ion-pair gave expected analytical and spectroscopic data consistent with their structures, cf. Experimental Section. Due to their strong hygroscopic nature, only freshly recrystallized ion-pairs were employed for vesicle preparation and subsequent characterization by different physical techniques.

Packing Parameter Calculations. It remains an intriguing question why certain amphiphiles form vesicles and others form micellar or other nonvesicular aggregates. This question has been theoretically addressed in the literature by Israelachvilli,[17] in particular. An

(13) (a) Fukuda, H.; Kawata, K.; Okuda, H.; Regen, S. L. *J. Am. Chem. Soc.* **1990**, *112*, 1635. (b) Kaler, E. W.; Murthy, A. K.; Rodrigueg, B. E.; Zasadzinski, J. A. N. *Science* **1989**, *245*, 1371.

(14) Bolaphiles (bolaamphiphiles), in contrast to their monopolar counterparts (single chain/single polar headgroup amphiphile), consist of two hydrophilic headgroups linked to the hydrophobic core in α,ω-position. See for reviews: (a) Escamilla, G. H.; Newkome, G. R. *Angew. Chem., Int. Ed. Engl.* **1994**, *33*, 1937. (b) Fuhrhop, J. H.; Bach, R. In *Advances in Supramolecular Chemistry*: Gokel, G. W., Ed.; JAI Press: Greenwich, CT, 1992; Vol. 2, pp 25−63.

(15) (a) De Rosa, M.; Gambacorta, A. *J. Mol. Biol.* **1985**, *182*, 131. (b) Gliozzi, A.; Rolandi, R.; de Rosa M.; Gambacorta, A. *J. Membr. Biol.* **1983**, *75*, 45.

(16) Bhattacharya, S.; De, S. *J. Chem. Soc., Chem. Commun.* **1996**, 1283.

Scheme 1[a]

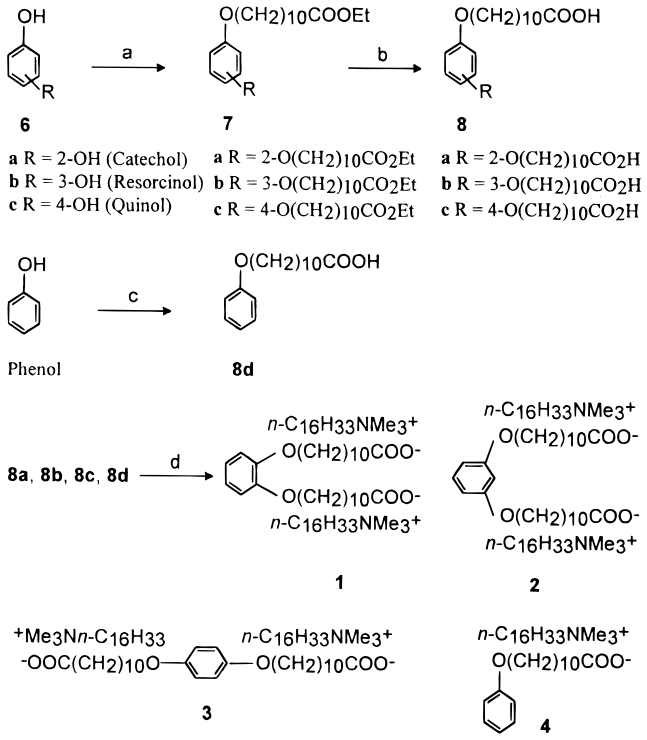

[a] Conditions. (a) $Br(CH_2)_{10}CO_2Et$, anhydrous K_2CO_3, acetone, reflux, 30 h, 85−90%; (b) aqueous KOH (5%), reflux, cool, aqueous acid, 80−85%; (c) i. $Br(CH_2)_{10}CO_2H$, NaOH (3.6 M), heat (~70 °C); ii. filter, acidification, 84%; (d) n-$C_{16}H_{33}N^+Me_3$, OH^- (2 equiv for **1**, **2**, and **3** and 1 equiv for **4**), MeOH, 25 °C, stir 24 h, 90−95%.

empirical rationale correlating molecular architecture with possible aggregate morphology has been extended by Israelachvilli,[18] Evans,[19] and Ninham.[20] According to this model, the critical packing parameter (p) is related to the geometric properties of the amphiphilic molecules by the equation v/la, where v is the volume of the hydrophobic chains of the amphiphile, l is the length of the hydrocarbon chain in its fully extended conformation, and a is the area of cross section occupied by the headgroup of an amphiphile at the aqueous interface.

Limiting areas of the condensed phases of a number of ion-paired systems have been experimentally determined[21] from the pressure−area diagram involving measurements in Langmuir balance. From the reported information, one can obtain an estimate of this cross-sectional area of the headgroup ion-pair $Me_3N^+\cdots{}^-O_2C$, as 68 ± 3 Å^2. We have used this area of cross section (a) for calculation of packing parameters of all the ion-pairs examined in the present study as all of them contain the $Me_3N^+\cdots{}^-O_2C$ ion-pair as headgroup. The amphiphile tail volumes (v) were obtained from the published[22] relationship, $v = (27.4 + 26.9n)$ Å^3, where n is the number of carbon atoms. The same was also calculated using the method of adding volume increments.[23] Both approaches were used in an effort to reduce ambiguity. The corresponding values for the hydrophobic chain length (l) were obtained from the equation $l = (1.5 + 1.265n)$ Å, where n is the number of carbon atoms. The lengths of the hydrocarbon segments of these ion-pairs in their fully extended conformation were also obtained from the calculation of energy-minimized conformations using the DISCOVER package of INSIGHT II (version 2.3.5, Biosym Technology Software). The values of hydrocarbon lengths obtained by either approach were in good agreement.

According to the above hypothesis, when the p value (v/la) falls between the limiting values of 0.5 and 1.0, vesicle formation is predicted. We obtained p values of ~0.6 ± 0.02 for **4** and ~0.56 ± 0.02 for **1**, **2**, and **3**. These orders of p values predict vesicle formation and agree with the experimental observations (see below).

Vesicle Formation. Encouraged by the results of the calculations of packing parameters, we then decided to examine the abilities of the ion-pairs toward vesicle formation by dispersal of these compounds in water. The aggregates were obtained by modified reverse phase evaporation method (REV).[24] A given ion-pair (2.5 mmol) was dissolved in 1 mL of $CHCl_3$. To this was added water (pH 6.8), and the two phase mixture was briefly bath-sonicated at ambient temperature to produce a stable emulsion. The organic solvent from that emulsion was reversibly evaporated under reduced pressure. The resulting suspension was then freeze-thawed several times. Then a brief bath-sonication above the phase transition temperature afforded stable, translucent vesicular aggregates.

For the fluorescence, UV−vis spectroscopy, and the X-ray diffraction studies, the vesicles were generated as follows. A dry lipid film was hydrated by keeping it in the presence of water for 12 h. Then the mixture was dispersed by vortexing for a few minutes followed by 5−6 freeze−thaw treatments. For the trapping experiments, the vesicles were formed by sonicating the screw-cap vials containing the required amount of the lipid and water having the fluorescence probe in a bath sonicator at ~60 °C or higher for 30 min. Vesicles prepared by either protocol remained optically stable for several days except that of **4**, as judged by their turbidity measurements at 450 nm, as a function of time.

Electron Microscopy. To confirm the formation of vesicular aggregates from this new series of synthetic, ion-paired systems, all the aggregates were examined under transmission electron microscopy (TEM) using a JEOL-TEM 200 CX instrument. For the TEM studies, the vesicles were generated by the REV method as described in the preceding section except that uranyl acetate was also included in the water in which the vesicles were formed. TEM examination of the air-dried, individual aqueous suspensions of **1**−**4** dried on carbon−Formvar coated copper grids revealed the existence of *closed* aggregate structures in all the cases (Figure 1). While, **1**, **2**, and **3** formed predominantly multilamellar spherical vesicles having diameters of 500−525 Å, 950−1000 Å, and 1200−1300 Å, respectively, vesicles from **4**, in contrast, formed predominantly unilamellar spheres

(17) Israelachvilli, J. N. *Intermolecular and Surface Forces*, 2nd ed.; Academic Press: New York, 1992.
(18) Israelachvilli, J. N.; Mitchell, D. J.; Ninham, B. W. *J. Chem. Soc., Faraday Trans.* **1976**, *72*, 1525.
(19) Mitchell, D. J.; Ninham, B. W. *J. Chem. Soc., Faraday Trans. 2* **1981**, *77*, 601.
(20) Evans, D. F.; Ninham, B. W. *J. Phys. Chem.* **1983**, *87*, 5025.
(21) (a) Shibata, O. *J. Colloid Interface Sci.* **1983**, *96*, 182. (b) Kaneshina, S.; Nakamura, M.; Matuura, R. *J. Colloid Interface Sci.* **1983**, *95*, 87.
(22) Tanford, C. *J. Phys. Chem.* **1972**, *76*, 3020.
(23) Kitaigorodsky, A. I. *Molecular Crystals and Molecules*; Academic Press: New York, 1973.
(24) DuZguenes, N.; Wilschut, J.; Hong, K.; Fraley, R.; Perry, C.; Friend, D. S.; James, T. L.; Papahadjopoulos, D. *Biochim. Biophys. Acta* **1983**, *732*, 289.

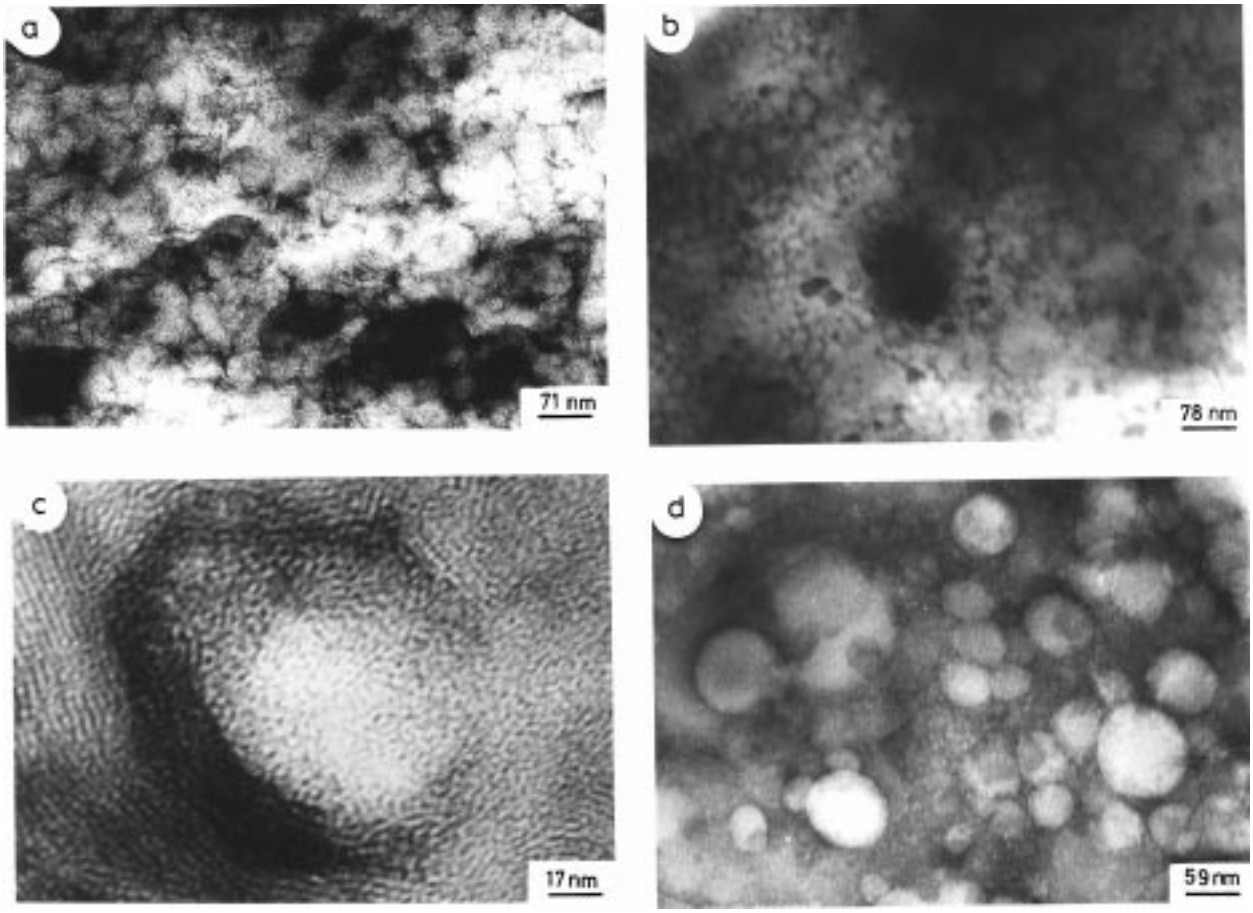

Figure 1. Uranyl acetate stained transmission electron micrographs of vesicles prepared by REV of **1**−**4**: (a) **1**, (b) **2**, (c) **3**, and (d) **4**.

having diameters ranging from 750 to 800 Å. Closer scrutiny of the micrographs shows that with vesicles of **1** the width of each lamellae ranged from ∼42 to 52 Å. Similarly vesicles of **3** had a lamellar width of ∼34.5 Å on average. These results are consistent with the XRD measurements on the cast films from the aggregates of the corresponding ion-pairs (see below). However, the information on the lamellar widths of vesicular **2** and **4** were not obvious.

Dynamic Light Scattering. Mean hydrodynamic diameters were determined by laser light scattering. Each suspension was generated by the reverse-phase evaporation method and examined for its ability to scatter. The mean hydrodynamic diameters were 600 ± 50 Å, 1000 ± 70 Å (>97%), 1400 ± 50 Å (>95%), and 800 ± 20 Å for **1**, **2**, **3**, and **4**, respectively. Minor populations with suspensions of **2** and **3** (<3 and <5%, respectively) consisting of larger aggregates (>2000 Å) were also seen.

Entrapment of Fluorescent Dye in Vesicles. After having confirmed the formation of vesicles from these newly developed ion-paired systems, we then decided to examine whether these vesicles were closed and in that situation whether these can sustain transmembrane ion gradients. Such an expectation is based on the fact that closed vesicles have the capacity to hold hydrophilic molecules or ions inside their inner aqueous cavity. In the entrapped situation, these solutes cannot permeate across the lipidic bilayers freely.

The membrane permeability can be measured with suitable water soluble markers. Although methods based on radiochemical, redox, or enzymatic techniques are well-documented in literature, method utilizing the fluorescence probe are widely used due to their simplicity and convenience.[25] A number of probes such as pyranine,[26] carboxyfluorescein,[27] calcein,[28] etc. have been used to estimate membrane permeability. However, due to their ionic nature it is possible that any of these could compete for ion-pairing during such experiments. Due to this concern we preferred to employ riboflavin, a neutral water soluble molecule which is strongly fluorescent in its neutral form but becomes nonfluorescent upon deprotonation ($pK_a \sim 10$). It can also withstand low ionic strength and, as a result, can be studied even in water alone. The usefulness of riboflavin has already been demonstrated independently by Kunitake,,[29] Regen,[13b] and Bhattacharya[11b] for the estimation of entrapment capacity and for the determination of transmembrane pH gradients with unrelated vesicle forming surfactants of diverse surface charges.

We first generated vesicles by dispersal of **1**−**5** (concentration 1 mg/1 mL) in a bath sonicator at ∼60 °C over a period of ∼30 min in water (pH 6.8) containing riboflavin (2×10^{-5} M). Sonication up to 30 min produced a translucent suspension, the turbidity (400 nm) of which did not change upon additional sonication.

(25) Brunner, J.; Graham, D. E.; Hauser, H.; Semenza, G. *J. Membr. Biol.* **1980**, *57*, 133.
(26) Kano, K.; Fendler, J. H. *Biochim. Biophys. Acta* **1978**, *509*, 289.
(27) (a) Neumann, R.; Ringsdorf, H.; Patton, E. V.; O'Brien, D. F. *Biochim. Biophys. Acta* **1987**, *898*, 338. (b) Weinstein, J. N.; Yoshikami, S.; Henkart, P.; Blumenthal, R.; Hagins, W. A. *Science* **1977**, *195*, 489.
(28) Matzuzaki, K.; Harada, S.; Funakoshi, N.; Fujii, K.; Miyajima, K. *Biochim. Biophys. Acta* **1991**, *1063*, 162.
(29) Kunitake, T.; Okahata, Y.; Yasunami, S. *Chem. Lett.* **1981**, 1397.

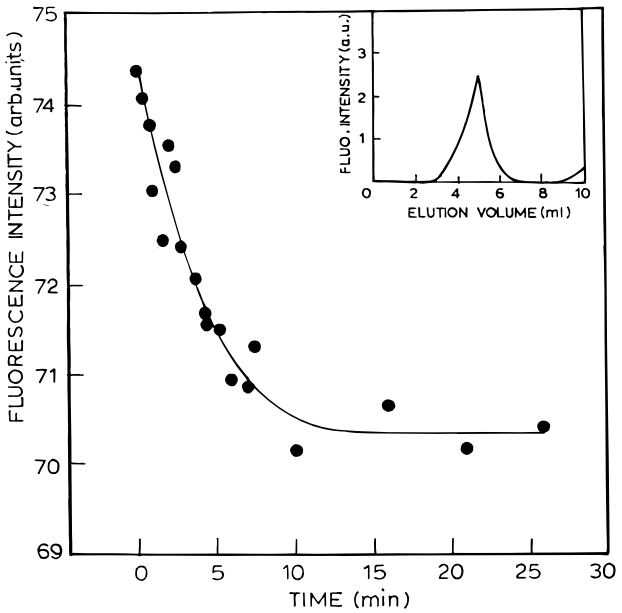

Figure 2. OH^- permeability profile of riboflavin entrapped vesicular **3**; inset shows the gel filtration profile of the dye entrapped vesicles of **3** using a Sephadex G-50 column.

The resulting vesicular suspension was loaded onto a Sephadex G-50 column, and gel filtration was performed to separate vesicle entrapped riboflavin from the free riboflavin. A representative gel filtration profile of the separation of free riboflavin from that bound at the membrane surface and also the riboflavin that is entrapped in vesicles was shown in Figure 2 (inset). Except with **1** and **4**, riboflavin-entrapped vesicles could be separated out. We suspect that the vesicles of **1** and **4** are so leaky that the encapsulated dye could not be sustained in the aqueous cavities of these vesicles. This leakiness could be due to the structural flaws and defects associated with the bilayers of these ion-paired systems (see below).

Kinetics of Transmembrane Permeation. The fluorescence emission due to the membrane-bound and entrapped riboflavin was measured at 514 nm upon excitation at 374 nm at 25 ± 0.5 °C. This includes the dye molecules that were adsorbed on the outer membrane surfaces and the ones that were entrapped within the inner water pools. As the pH of the vesicle dispersion was raised from 6.8 to 10.2, the fluorescence intensity (514 nm) decreased initially "instantaneously" to about 78 ± 5% of the original value (recorded prior to pH adjustment). We attribute this immediate ca. 22 ± 5% loss in the fluorescence intensity to the deprotonation of riboflavin molecules that are bound at the outer surfaces of the vesicles. At the exposed exovesicular surfaces, riboflavin molecules underwent instantaneous ionization as the pH was increased. The residual fluorescence intensity, however, disappeared as a function of time for vesicular **3** (Figure 2). Since the residual loss in fluorescence intensity was time-dependent, we calculated the half-time of this process ($t_{1/2}$ ~3.2 min, k_{perm} ~3.6×10^{-3} s^{-1}) (Table 1). The fraction of the entrapped riboflavin was ~0.82%. Time-dependent loss of the fluorescence intensity due to the conversion of neutral riboflavin into its deprotonated form upon pH adjustment (6.8 → 10.2) demonstrated that it contained an internal aqueous compartment. Taking a bilayer thickness of ~35 Å for vesicles of **3** based on TEM and XRD results and assuming the time-dependent loss of riboflavin fluorescence as a rate-limiting permeation of exovesicular OH^- into the vesicle's interior aqueous compartment, we calculate P to be ~1.9×10^{-8} cm/s for the permeation constant of OH^- toward vesicles at pH 10.2.

Table 1. Riboflavin Entrapment and Estimated OH^- Permeability in Different Bilayer Membranes from Ion-Paired Systems 1−4 at 25 °C[a]

lipid	lipid concn (mM)	% entrapment[b]	$10^3 k_{perm}$ (s^{-1})	$10^8 P$[c,d] (cm/s)
1	0.96	*e*		
2	0.96	2.28	*f*	
3	0.96	0.82	3.6	1.9
4	1.78	*e*		

[a] The time-dependent decay of the fluorescence intensity at 514 nm was monitored as a function of time. The decay process followed apparent pseudo-first-order kinetics. The rate constant values represent averages of three independent experiments, and the reproducibility was ±4%. In each case, the extent of fluorescence decay was followed beyond 90% and the decay followed an apparent pseudo-first-order rate constant. [b] The entrapment of riboflavin given in percentages has been corrected for an apparent absorption of marker molecules in each case. [c] Calculated on the basis of diameters obtained in transmission electron microscopy. [d] Bilayer thicknesses have been obtained from the X-ray diffraction studies. We also interpret the time-dependent loss of fluorescence intensity as a permeation-limited deprotonation of riboflavin entrapped in the internal aqueous compartment of OH^-. [e] Vesicles did not entrap any dye. [f] The fluorescence loss in this case was "instantaneous".

In the case of vesicular **2**, the initial fluorescence intensity underwent a rapid decay upon pH adjustment (6.8 → 10.2). However, the subsequent time-dependent loss of fluorescence in this instance was not observed. Presumably due to "loose" packing of the monomers of **2** in vesicles, the ionization of the riboflavin molecules that are adhering at the membrane outer surfaces and the transbilayer OH^- permeation occur simultaneously and could not be distinguished. Indeed the vesicles of **2** at 25 °C are in their fluid state as indicated by thermal phase transition studies (see below), and therefore one can further expect these bilayers to be rather disordered (and hence leaky) under the conditions of this study.

In contrast to the above situations, vesicular **1** and **4** did not show any evidence of riboflavin entrapment. Therefore these vesicles do not appear to have the binding ability at their outer surfaces nor do they have the capacity to sustain riboflavin molecules in their inner aqueous pools. It is not, however, obvious why these vesicles cannot bind or entrap the dye molecules especially when the TEM studies indicated the existence of closed aggregates from **1** and **4**.

Differential Scanning Calorimetry. To further ascertain the presence of lamellar organizations in such aggregates, the vesicles of the above ion-paired systems **1**−**5** were examined by differential scanning calorimetry (DSC). Since the presence of a small amount of impurity can affect the thermotropic properties and can also broaden the transition, all the ion-paired systems were recrystallized prior to calorimetric experiments. DSC heating and cooling scans were obtained from individual aqueous dispersions of the surfactants (120 mM, pH 6.8) in a Perkin-Elmer Model DSC-2C differential scanning calorimeter. Well-defined, sharp and single phase transitions were obtained for **3** (~85 °C) (Figure 3), **4** (~31 °C), and **5** (~42 °C) during heating runs. **4** and **5** showed almost reversible phase transition behavior during heating as well as cooling cycles. However, vesicles of **3** showed a lower transition (~61.5 °C) in the cooling run although a repeat heating run with the same sample of

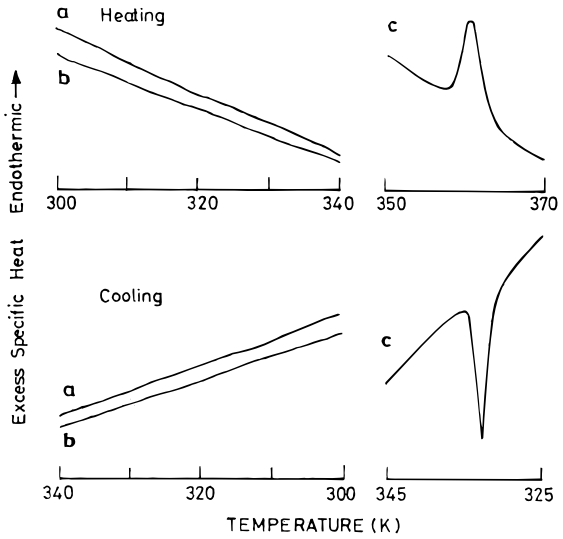

Figure 3. Gel to liquid-crystalline phase transition of the vesicles of the ion-paired lipids **1**−**3**: (a) **1**, (b) **2**, and (c) **3**.

Table 2. Gel to Liquid-Crystalline Main Phase Transition Properties for the Ion-Paired Amphiphiles 1−5 by Differential Scanning Calorimetry[a]

lipid	T_m (°C) heat	T_m (°C) cool	ΔH_{cal}[b] (kcal/mol)	ΔS[c] (cal/K·mol)	ΔH_{vH}[d] (kcal/mol)	CU[e] (molecules)
1	*f*	*f*				
2	*f*	*f*				
3	85.0	61.2	4.4	12.5	330.1	75
4	31.3	29.1	5.34	17.55	213.7	40
5	41.6	40.2	6.0	19.1	600.5	100

[a] Concentration of gel was 120 mM. [b] The ΔH_{cal} values quoted are the average of the total enthalpy for successive runs. We estimate that transition enthalpies are accurate to ±0.5 kcal mol^{-1}. [c] ΔS values were calculated by dividing $\Delta H_{cal}/T_m$ assuming the phase transition as a first-order process. [d] ΔH_{vH}, van't Hoff enthalpy values, were calculated from the relation $\Delta H_{vH} = 6.9T_m^2/\Delta T_{1/2}$, where $\Delta T_{1/2}$ is the spread of temperature at half-height.[e] The CU values are the average for successive runs. [f] No detectable transition at this concentration (see text for details).

vesicular **3** reproduced the thermogram with T_m at ∼85 °C. Notably the corresponding dispersions from **1** and **2** did not, however, show any detectable transition in the temperature region 25−90 °C either in the heating or in the cooling thermograms (Figure 3). The phase transition temperatures (T_m), calorimetric enthalpies (ΔH_{cal}), van't Hoff enthalpies (ΔH_{vH}), and cooperativity units are given in the Table 2.

Microcalorimetry. Examination of the corresponding vesicles at lower concentration (2.5 mM) using microcalorimetry reproduced the peaks related to T_m for **4** and **5** as obtained under DSC at 120 mM concentration. However, with **3**, the cooperativity was drastically reduced at 2.5 mM concentration. Strikingly, the vesicles of **1** at this concentration (2.5 mM) now gave a pronounced peak at ∼39 °C under microcalorimetry in contrast to what was observed under DSC at higher (120 mM) concentration. Vesicular **2**, however, still did not show any detectable peak in the temperature range 22−90 °C, consistent with what was observed with suspensions of **2** at higher concentration (120 mM) under DSC. These results indicated that thermal meltings of some of these bilayers do indeed depend on concentrations which may find their origin in the formation of various types of aggregates that include SUV, LUV, and MLV's.

Fluorescence Anisotropy Measurements. To probe the apparent concentration dependence observed with

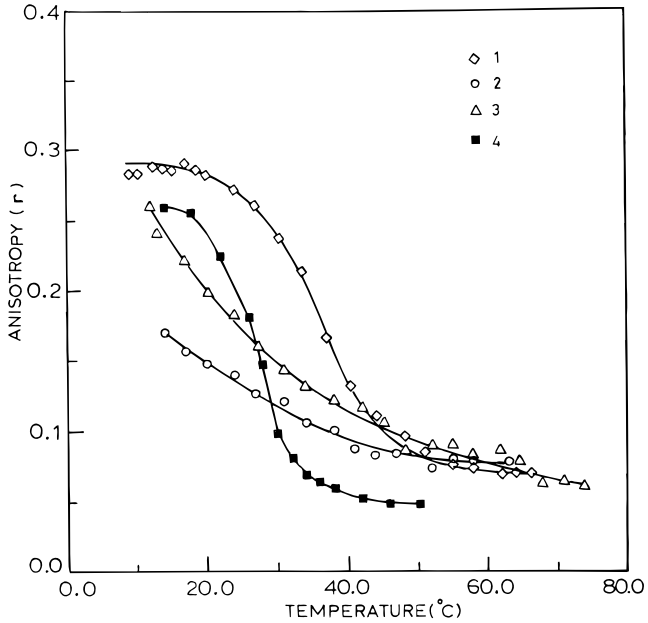

Figure 4. Fluorescence anisotropy (r) vs temperature (°C) plots for different lipid vesicles.

Table 3. Phase Transition Temperatures (T_m/°C) of Vesicular 1−5 by Microcalorimetry, Fluorescence Anisotropy, and UV Method. Fluorescence Anisotropy (r) at 15 °C and I_1/I_3 at 25 and 50 °C Are Also Given for Comparison[a]

lipid	main transition[b] (°C) microcal.	main transition[b] (°C) fluor. ani.	main transition[b] (°C) UV method	anisotropy (r) at 15 °C	I_1/I_3 at 25 °C	I_1/I_3 at 50 °C
1	39.1	37.0	38.0	0.29	0.98	0.93
2	*c*	*d*	12.0	0.17	0.97	0.93
3	84.9	*e*	*f*	0.24	0.93	0.89
4	35.3	30.5	*g*	0.26	1.24	0.93
5	41.8	41.0	42.0	0.3	1.26	0.93

[a] Concentration of vesicular solutions in all the cases was 2.5 mM. [b] Average deviation is ±0.5 °C for microcalorimetry, ±1 °C for fluorescence anisotropy method, and ±2 °C for UV method. [c] No detectable transition. [d] No break in r vs T plot. [e] Broad transition. [f] No maxima and break in A_{enol}/A_{keto} vs T plot. [g] Not determined.

vesicular **1** and **3**, we then measured the fluorescence anisotropy as a function of temperature. This technique has been extensively used for probing the fluidity of the interior of the vesicle bilayer and for measuring the temperature (T_m) at which the bilayer undergoes a transition from a gel-like to a liquid-crystalline state.[30] We have measured the fluorescence anisotropy (r) as a function of temperature (in the range 10−75 °C) using 1,6-diphenylhexa-1,3,5-triene (DPH), a hydrophobic fluorescent probe which intercalates between the alkyl chains in the core of the vesicle bilayer.

The anisotropy sensed by DPH in respective membranes is a function of the membrane fluidity. Thus, the relationship of steady-state fluorescence anisotropy (r) of DPH and temperature was utilized to evaluate the relative fluidity and phase transition behaviors of the lipid membranes (Figure 4). Fluorescence anisotropy values and phase transition temperatures for 2.5 mM **1**−**5** are included in Table 3.

As is evident from Figure 4, the vesicular solutions showed rather well-defined and cooperative phase transi-

(30) (a) Andrich, M. P.; Vanderkooi, J. M. *Biochemistry*, **1976**, *15*, 1257. (b) Shinitzky, M.; Barenholz, Y. *Biochim. Biophys. Acta* **1978**, *515*, 367.

Table 4. Comparison of Unit Layer Thicknesses Obtained from X-ray Diffraction of Self-Supporting Cast Films and Molecular Modeling Studies

	unit layer thickness (Å)	
lipid	obsd[a]	calcd[b]
1	46.8	44.0, 33.0
2	39.1	39.0, 33.7
3	36.1	34.5
4	33.4	40.5
5	37.9	41.0

[a] As obtained from reflection XRD of cast films. [b] Molecular lengths of unit layers of ion-pairs as estimated from energy-minimized CPK models (INSIGHT).

tions in the cases of **1**, **4**, and **5**. In contrast the corresponding thermograms were broader in the cases of **2** and **3** and did not show clear evidence of breaks related to T_m. Further examination of Figure 4 reveals that the fluorescence anisotropy value (r) at 15 °C was quite different for **2** ($r = 0.17$) than that for **1**, **3**, **4**, and **5** ($r = 0.24-0.29$) although there was little difference in the polarization values after the phase transitions. Since the anisotropy is directly related to microfluidity of bilayers, the above observation suggests that the bilayers of **2** are already in the fluid state at 15 °C. DPH is a lipophilic molecule and locates only in the hydrophobic center of the bilayer membrane. Therefore, the decrease in the anisotropy value indicates the higher movement of DPH in the bilayers of **2**, i.e., the intramonomer van der Waals interactions between the chains in **2** are severely "loose". The bilayers of **1**, **3**, **4**, and **5** are considerably more rigid at this temperature and should therefore be in their gel-like solid states. Note, however, that the thermogram in the case of **3** was really broad and hence the transition is quite noncooperative at this concentration (2.5 mM). This observation is consistent with the results obtained at the same concentration in microcalorimetry where although the transition was seen, it was quite poor in cooperativity (not shown). It is difficult to rationalize all of the above observations. However, noncooperativity has been observed previously[31] for bolaform amphiphiles having a membrane spanning spacer, probably due to the presence of gaps in the outer leaflets of the vesicles. We believe that this could be one possible explanation why **3** shows poor cooperativity in its thermotropic phase transition. In addition, the increased rigidity offered by quinol-based structural segments in **3** might also cause apparent mitigation of cooperativity in the thermal phase transition of these bilayers.

Temperature-Dependent UV Spectral Variations with Vesicle-Doped BAA. Benzoylacetanilide (BAA) is a water soluble molecule that undergoes keto−enol tautomerism. Ueno used this as a probe for the determination of apparent thermal phase transition temperature (T_m) of various bilayer membranes.[32] To further examine the concentration dependent melting behavior of these ion-paired systems, we used the same probe in our studies. However, vesicular **4** and **5** were not examined using this method since well-defined DSC profiles were obtained for both of them irrespective of their concentrations.

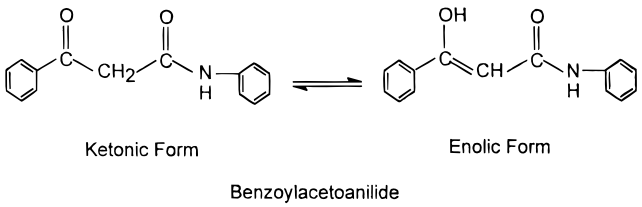

Benzoylacetoanilide

An optically clear BAA-doped vesicular solution (1×10^{-3} M) was first prepared. The absorbance maxima due to the vesicle-doped enol and keto forms of BAA were indicated at 315 and 250 nm, respectively. The ratio [A_{enol}/A_{keto}] was found to increase sharply during the phase transition of the bilayers, and the maximum was seen at T_m.[32] Then it decreased as the temperature increased beyond T_m. The vesicular solutions of **1**−**3** were studied in the temperature range of 6−70 °C. The temperature (T_m) related to the melting of "frozen" gel-like state to "fluid" liquid-crystalline state, as measured by using tautomerism of vesicle-doped BAA was found to be comparable with corresponding values obtained by the determination of fluorescence anisotropy as a function of temperature. Sharp maxima obtained (Figure 5) from the plot of [A_{enol}/A_{keto}] with temperature for **1** and **2** were at 38 and 12 °C, respectively. Similarly, upon cooling they showed a single break within ±2 °C of the respective T_m values observed during heating runs. BAA-doped vesicles of **3** did not show any maxima in the temperature range studied (10−60 °C). These findings further confirm the concentration dependent modulation of the phase transition properties of the membranes of **1**−**3**.

Micropolarity and Phase Transition Temperature by Pyrene. To secure additional and independent confirmation of the observed concentration dependence, we also measured the monomer vibrational intensity ratio (I_3/I_1) of bilayer-doped pyrene as a function of temperature. This method has been widely used to determine the apparent T_m from the break of the I_3/I_1 vs T plot for various lipid dispersions.[33] The relevant data are summarized in Table 3. In the cases of **4** and **5**, I_3/I_1 vs T gave sigmoidal plots as expected, i.e., I_3/I_1 value sharply increased during the phase transition and then became constant (1.06−1.07) (figure not shown). In the cases of **1** and **2**, the I_3/I_1 vs T plot gave straight lines with positive slopes in the temperature region 15−50 °C. No break was obtained. In case of **3**, I_3/I_1 vs T gave a broad, noncooperative transition. But strikingly, the four vesicular solutions that contain an aromatic ring in their ion-pairs showed different I_3/I_1 values at room temperature (25 °C) which suggested differences in the micropolarities of the vesicular solutions. Probably the emission due to pyrene probes interfered with the aromatic units in lipids which might be responsible for lack of any break in the I_3/I_1 vs T plot related to apparent T_m of these vesicles.

The value of I_1/I_3 depends on the chemical composition of the medium surrounding the probe and, thus, gives an estimation of the micropolarity of the surrounding medium. Table 3 showed the I_1/I_3 values of **1**−**5** at 25 and 50 °C. It prompted us to believe that the local composition at the vesicle solubilization site of pyrene is different depending on the nature of the substitution of alkyl chain on the aromatic unit. The value of I_1/I_3 is

(31) (a) Duivenvoorde, F. L.; Feiters, M. C.; van der Gaast, S. J.; Engberts, J. B. F. N. *Langmuir*, **1997**, *13*, 3737. (b) Fuhrhop, J.-H.; Liman, U.; Koesling, V. *J. Am. Chem. Soc.* **1988**, *110*, 6840.

(32) Ueno, M.; Katoh, S.; Kobayashi, S.; Tomoyama, E,; Obata, R.; Nakao, H.; Ohsama, S.; Koyama, N.; Morita, Y. *Langmuir* **1991**, *7*, 918.

(33) Kalyanasundaram, K. *Photochemistry in Microheterogeneous Systems*; Academic Press: New York, 1987; p 177.

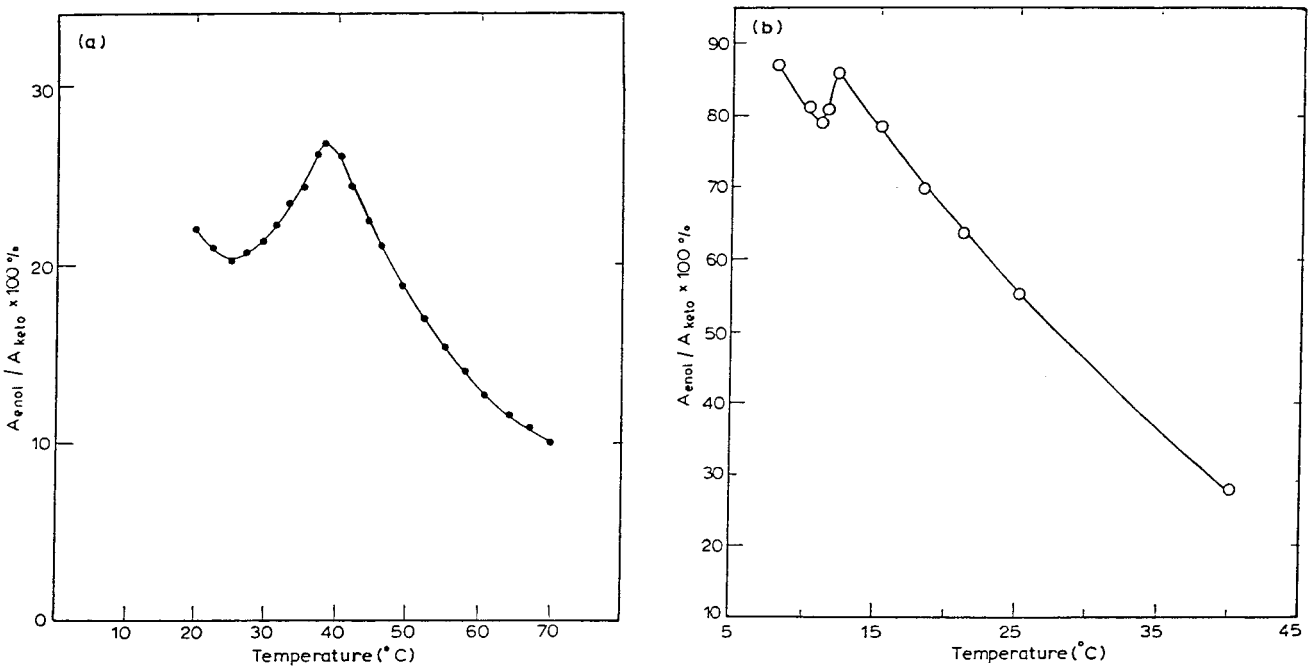

Figure 5. Plots of A_{enol}/A_{keto} due to vesicle-doped BAA vs temperature (°C) for (a) **1** and (b) **2**.

significantly different for **1**−**3** (0.97) compared to that of **4** and **5** (∼1.25) at 25 °C where all but **2** are present in their gel states. Pyrene sensed more hydrophobic microenvironments in **1**−**3** compared to that in **4** at 25 °C. This indicates that instead of residing near the interfacial region of the vesicle, pyrene localizes itself near the aromatic ring embedded in the hydrophobic membrane core probably due to more favorable aromatic−aromatic interactions.

UV−Vis Studies. To examine whether there is any existence of interaromatic stacking interactions in such aggregates, we then proceeded to compare their UV−vis spectra in organic solvent with that of aggregates in water. The absorption peaks for **1** and **4** in $CHCl_3$ appeared at 241.8 and 278.6 nm and 242.5, 272.8, and 278.8 nm, respectively. The corresponding absorption maxima for vesicular **1** and **4** were 228.0, 274.8, and 278.6 nm and 227.8, 272.5, and 278.7 nm, respectively (Figures 6b and 6a). Thus, with **1** and **4**, the UV−vis spectra in $CHCl_3$ and in vesicular solutions were quite similar. On the other hand, the absorption peaks for **2** in $CHCl_3$ occurred at 241.4, 276.6, and 282.5 nm (shoulder peak), respectively, which shifted to 226.0, 275.2, and 281.6 nm in aqueous dispersion (Figure 6c). Similarly, the absorption peaks for a solution of **3** in $CHCl_3$ occurred at 241 and 292.8 nm, but for the corresponding vesicular dispersion, the absorption maxima were located at 226.0, 294.0, and 302.0 nm (Figure 6d). Thus, in the case of **3**, a red shift as large as 10 nm and, for **2**, a 3 nm red shift were observed in vesicular solutions when compared to the respective spectra taken in $CHCl_3$.

According to the molecular exciton model,[34] the red shift observed for the bilayer aggregate should be derived from the π-stacking of the chromophore, which has also been defined as the *J*-like aggregation.[35] It is also attributable to a tilted chromophore orientation. Therefore, these studies clearly show the existence of the aromatic−aromatic stacking interaction between the aromatic rings in **3** and to a limited extent in **2** while they are in their aggregated vesicular form. No such indications were, however, apparent from the vesicles of **1** or **4**.

X-ray Diffraction Studies. To understand the orientation of these ion-paired systems in the membranes and also to gain knowledge about their lamellar packing, X-ray diffraction studies were performed on supported, cast films of **1**−**5**. Reflections up to 20° were analyzed and interpreted in terms of higher order reflections of stacked bilayer structures.[36]

A series of reflections mostly up to the eighth order reflections were obtained (not shown) for **1**−**4** and **5**, the highest intensity peak corresponding to the lowest 2θ value being the long spacing. The long spacings were 46.8, 39.11, 36.06, and 33.41 Å for **1**−**4**, respectively on the basis of the higher order reflections (n = 3, 4, 5, 6, 7). Closer examination of the scan profiles also showed the existence of another series of very weak reflections presumably indicating the presence of a second kind of molecular packing in these aggregates. The X-ray diffraction of **5** was run for comparison which gave the long spacing value of 37.85 Å. When we extended the studies in the low angle range, we identified a weak reflection at 1.74°, corresponding to a *d* spacing of 50.85 Å. These diverse long spacing values clearly indicate the formation of different kinds of aggregates by these amphiphiles in aqueous dispersions which is in agreement with observed differences in the UV−visible spectra taken in $CHCl_3$ and in aqueous dispersions.

Assuming the long hydrocarbon and the fatty acid chains in these amphiphiles to have a *s*-trans conforma-

(34) Kasha, M. In *Spectroscopy of Excited State*; Plenum Press: New York, 1976; p 337.

(35) (a) Tai, Z.; Qian, X.; Wu, L.; Zhu, C. *J. Chem. Soc., Chem. Commun.* **1994**, 1965. (b) Everaars, M. D.; Marcelis, A. T. M.; Sudhölter, E. J. R. *Langmuir* **1993**, *9*, 1986.

(36) (a) Kimizuka, N.; Kawasaki, T.; Kunitake, T. *J. Am. Chem. Soc.* **1993**, *115*, 4387. (b) Kunitake, T.; Shimomura, M.; Kajiyama, T.; Harada, A.; Okuyama, K.; Takayanagi, M. *Thin Solid Films* **1984**, *121*, L89.

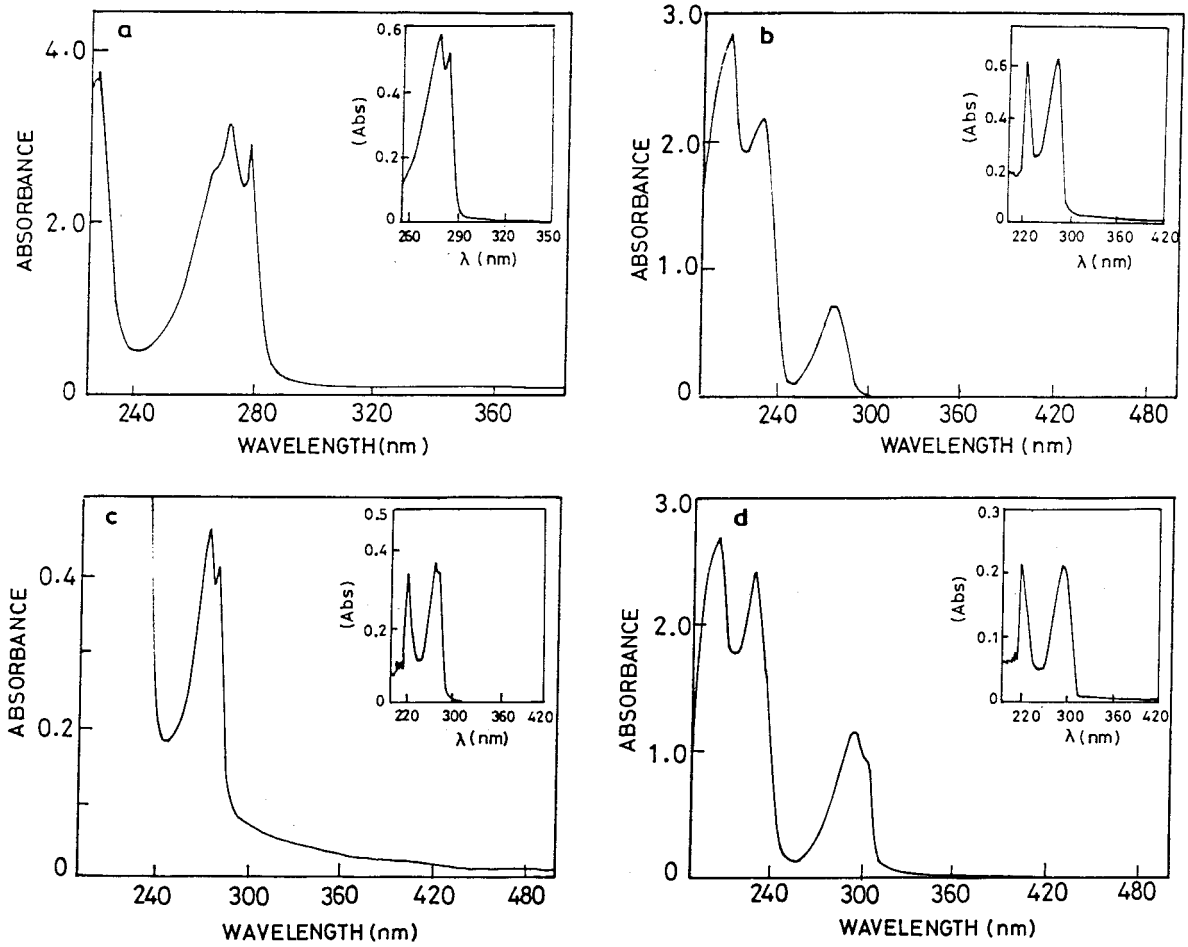

Figure 6. Comparison of UV−vis spectra in aqueous dispersion of (a) **4**, (b) **1**, (c) **2**, and (d) **3**; inset shows the corresponding UV−vis spectra in $CHCl_3$.

tion, the thicknesses of the bilayers corresponding to **4** and **5** were estimated to be ~ 41 Å from a CPK model of two respective molecules oriented parallel to the bilayer normal. The measured values of 33.41 and 37.85 Å, respectively, suggest a tilted bilayer arrangement of the alkyl tails. In the case of **1**, i.e., with the counterion anchoring through an ortho-substituted aromatic ring, a folded arrangement with two hydrophobic chains pointing to one direction is possible and thus gives rise to a bilayer type orientation. In case of **2**, the meta-oriented isomer supports the interdigitated mode of packing. In contrast, **3** with para directionality allows the spanning of the undecanoate chains to opposite directions in the membrane and thus the unit layer thickness is very close to the length of the corresponding bolaphile.

Molecular Modeling Studies. To rationalize the possible origin of such variations of the biophysical properties of vesicular **1**−**5**, depending on the geometric features of the bolaphilic segments in these ion-pairs we also carried out molecular mechanics studies. All the ion-pairs were drawn in the computer using INSIGHT II,[37] and their energies were minimized (see Supporting Information). In **1**, the two apolar undecanoate chains in the bolaphilic core originate from a central catechol unit and are at ~60° in their extended conformations. Even after ion-pairing, chain propagation in **1** in an angular fashion leads to severe packing impairment. In addition, as indicated from molecular modeling, other conformational plans (tilted) are also possible to minimize apolar chain/water contacts. It may be possible that a number of such arrangements could coexist leading to concentration dependent phase transition behavior. With **2**, the undecanoate chains stem from a central resorcinol unit and remain at an angle of ~120°. In the conformational plan with a unit layer thickness of ~39 Å (consistent with the value obtained from the reflection X-ray diffraction experiment on the cast film of **2**), the intramonomer van der Waals interactions between the chains become severely "loose". Variation of its concentration may lead to the formation of alternative structures. Indeed XRD studies with cast films of aggregates of **2** also indicated the existence of additional organizations. Despite the presence of structural "flaws" in the bolaphilic core of **2**, the self-assembly of ion-pair persists in such a way that a lower phase transition temperature (<15 °C) is manifested. In contrast, the presence of an aromatic quinol moiety at the bolaphilic core of **3** allows the formation of tightly organized assemblies as the undecanoate chains from the central quinol units span along opposite directions (~180°). This conformational plan gives optimal van der Waals contacts upon ion-pairing with CTA^+ and also interaromatic π-stacking association. The existence of a stacking type of interaction is supported by a comparison of the UV−vis

(37) For details please consult BIOSYM programs, which are available from Biosym Technologies, 9685 Scranton Road, San Diego, CA 92121-3752.

studies of the aqueous aggregates of **3** against its solution in $CHCl_3$. It is difficult to explain the observed effect on dilution of **3** on the basis of molecular mechanics calculations alone. Presumably dilution to lower concentration leads to the formation of other plans that may not support bilayer type organization. Whatever may be the exact reason, the present observations are novel and unprecedented and also show for the first time that the vesicle formation could be controlled by variation of concentration.

In summary we have synthesized four new gemini carboxylate surfactants and their corresponding ion-pairs with CTA^+ which upon dispersion in water afforded vesicular aggregates. Detailed examination of their morphological and biophysical properties by a variety of physical methods indicates that it is possible to modulate their finer bilayer organizations which in turn affect their properties at the membranous levels. Present findings illustrate a novel approach to fine-tuning vesicular properties and suggest new recipes for stable vesicular structures that may be of practical value. In particular, mixed bilayers composed of bacterial lipid (bolaamphiphile) and fatty acids or mammalian lipids (monopolar amphiphile) like cardiolipins could be tailored to have useful biological properties. Some of these mixtures may also produce transient membrane-like milieu. These aspects are currently under examination.

Experimental Section

General. Melting points were recorded in open capillaries and are uncorrected. NMR spectra of $CDCl_3$ solutions were obtained at 90, 200, or 270 MHz (^1H). Descriptions of instruments used for various characterizations have been published.[7a]

Cetyltrimethylammonium bromide (CTAB), 11-bromoundecanoic acid, 1,6-diphenyl-1,3,5-hexatriene (DPH), riboflavin, pyrene, and Amberlite IRA-900 (OH^- form) were from Aldrich Chemical Co. Benzoylacetanilide (BAA) was prepared by the dropwise addition of aniline to ethyl benzoylacetoacetate at 150 °C in xylene. Phenol was distilled, and catechol, resorcinol, and quinol were used after purification. Thin-layer chromatography was performed on Merck silica gel-G plates. Column chromatography was performed on silica gel (60−120 mesh, Merck). All the reagents and solvents were the highest grade available commercially and used purified, dried, or freshly distilled as required.

Synthesis. The syntheses of four ion-paired amphiphiles are described below.

Diethyl Phenyl-1,2-bis(oxyundecanoate) (7a). A mixture of catechol (0.66 g, 6.0 mmol), ethyl bromoundecanoate (3.52 g, 12.0 mmol), and fused potassium carbonate (5.4 g, 40 mmol) in 50 mL of dry acetone was refluxed for 18 h until TLC indicated the disappearance of the spot due to catechol. The insoluble solid residue from the reaction mixture was removed by filtration, and the filtrate was concentrated. The residue obtained on evaporation of acetone was chromatographed over silica gel with hexane/EtOAc (98:2) to give **7a** (2.88 g, 90%) as a white solid: mp 40−41 °C; TLC (hexane/EtOAc 10:1); R_f 0.75; ^1H NMR ($CDCl_3$, 90 MHz) δ 1.12−2.0 (m, 38H), 2.25 (t, 4H), 4.0 (t, 4H), 4.12 (q, 4H), 6.88 (s, 4H); ^{13}C NMR ($CDCl_3$, 22.5 MHz) δ 14.30, 25.03, 26.00, 29.36, 34.35, 60.13, 69.24, 75.74, 77.14, 78.55, 114.2, 121.03, 149.3, 173.79; IR (Nujol) 1730, 1250 cm^{-1}; LRMS, EI, *m/z* (%) 534 (62); HRMS (EI) calcd for $C_{32}H_{54}O_6$ 534.4206, found 534.3921. Anal. Calcd for $C_{32}H_{54}O_6$: C, 71.87; H, 10.18. Found: C, 71.78; H, 10.11.

Phenyl-1,2-bis(oxyundecanoic acid) (8a). 7a (0.3 g, 0.56 mmol) was heated with potassium hydroxide (0.4 g, 8.7 mmol) in ethanol (10 mL) on a water bath for 5 h. Excess ethanol was removed, the residue obtained was diluted with water (20 mL), and the mixture was filtered. Acidification of the clear filtrate gave the corresponding diacid (**8a**) as white crystals (0.22 g, 80%): mp 88−90 °C; ^1H NMR (DMSO-d_6, 90 MHz) δ 1.25−1.80 (s + "br" m, 32H), 2.25 (t, 4H), 3.98 (t, 4H), 6.88 (s, 4H); IR (Nujol) 1685, 1245 cm^{-1}; LRMS, EI, *m/z* (%) 478 (22). Anal. Calcd for $C_{28}H_{46}O_6$: C, 70.26; H, 9.68. Found: C, 70.31; H, 9.61.

Diethyl Phenyl-1,3-bis(oxyundecanoate) (7b). A mixture of resorcinol (0.27 g, 2.5 mmol), ethyl 11-bromoundecanoate (1.46 g, 5 mmol), and fused potassium carbonate (1.1 g, 8.0 mmol) in 25 mL of dry acetone was refluxed for 20 h. Then the reaction mixture was filtered, and upon evaporation of acetone from the filtrate a solid was obtained. It was chromatographed on silica gel with hexane/EtOAc (96:4) to give **7b** (1.14 g, 85%) as a white solid: mp 45−46 °C; TLC (hexane/EtOAc 4:1), R_f 0.8; ^1H NMR ($CDCl_3$, 90 MHz) δ 1.16−2.0 (m, 38H), 2.28 (t, 4H), 3.92 (t, 4H), 4.12 (q, 4H), 6.36−6.52 (m, 3H), 7.12 (t, 1H); ^{13}C NMR ($CDCl_3$, 22.5 MHz) δ 14.67, 24.44, 26.67, 34.67, 60.22, 68.0, 101.56, 106.67, 130.0, 160.67, 174.0; IR (Nujol) 1715, 1275 cm^{-1}; LRMS, EI, *m/z* (%) 534 (22); HRMS (EI) calcd for $C_{32}H_{54}O_6$ 534.4206, found 534.3921. Anal. Calcd for $C_{32}H_{54}O_6$: C, 71.87; H, 10.18. Found: C, 71.81; H, 10.13.

Phenyl-1,3-bis(oxyundecanoic acid) (8b). 7b (0.3 g, 0.56 mmol) was heated with potassium hydroxide (0.4 g, 8.7 mmol) in ethanol (10 mL) on a water bath for 5 h. Excess ethanol was removed, the residue obtained was diluted with water (20 mL), and the mixture was filtered. Acidification of the clear filtrate gave the corresponding diacid (**8b**) as white crystals (0.23 g, 85%): mp 119−121 °C; ^1H NMR (DMSO-d_6, 90 MHz) δ 1.25−1.80 (s + "br" m, 32H), 2.25 (t, 4H), 3.95 (t, 4H), 6.40−6.52 (m, 3H), 7.15 (apparent t, 1H); ^{13}C NMR ($CDCl_3$, 22.5 MHz) δ 24.89, 26.0, 29.11, 34.22, 67.78, 101.33, 106.89, 130.22, 160.67, 175.1; IR (Nujol) 1685, 1275 cm^{-1}; LRMS, EI, *m/z* (%) 478 (23). Anal. Calcd for $C_{28}H_{46}O_6$: C, 70.26; H, 9.68. Found: C, 70.21; H, 9.71.

Diethyl Phenyl-1,4-bis(oxyundecanoate) (7c). A mixture of quinol (0.66 g, 6 mmol), ethyl bromoundecanoate (3.52 g, 12 mmol), and fused potassium carbonate (2.7 g, 20 mmol) in 50 mL of dry acetone was refluxed for 24 h. The solvent was removed from the reaction mixture. This afforded a solid which upon chromatography on silica gel using $CHCl_3$ produced **7c** (2.76 g, 86%) as colorless crystals: mp 68−69 °C; TLC ($CHCl_3$), R_f 0.65; ^1H NMR ($CDCl_3$, 90 MHz) δ 1.0−1.92 (m, 38H), 2.28 (t, 4H), 3.88 (t, 4H), 4.12 (q, 4H), 6.8 (s, 4H); ^{13}C NMR ($CDCl_3$, 22.5 MHz) δ 14.44, 25.33, 26.44, 30.0, 34.44, 60.0, 68.44, 115.78, 153.56, 174.0; IR (Nujol) 1725, 1225 cm^{-1}; LRMS, EI, *m/z* (%) 534 (100); HRMS (EI) calcd for $C_{32}H_{54}O_6$ 534.4206, found 534.3998. Anal. Calcd for $C_{32}H_{54}O_6$: C, 71.87; H, 10.18. Found: C, 71.83; H, 10.08.

Phenyl-1,4-bis(oxyundecanoic acid) (8c). 7c (0.3 g, 0.56 mmol) was heated with potassium hydroxide (0.4 g, 8.7 mmol) in ethanol (10 mL) on a water bath for 5 h. Excess ethanol was removed, the residue obtained was diluted with water (20 mL), and the mixture was filtered. Acidification of the clear filtrate gave the corresponding diacid (**8c**) as white crystals (0.25 g, 90%): mp 128−130 °C; ^1H NMR (DMSO-d_6, 90 MHz) δ 1.25−1.80 (s + "br" m, 32H), 2.25 (t, 4H), 3.92 (t, 4H), 6.82 (s, 4H); IR (Nujol) 1695, 1230 cm^{-1}; LRMS, EI, *m/z* (%) 478 (20). Anal. Calcd for $C_{28}H_{46}O_6$: C, 70.26; H, 9.68. Found: C, 70.23; H, 9.69.

11-Phenoxyundecanoic acid (8d). To a mixture of freshly distilled phenol (1.41 g, 15 mmol) and 11-bromoundecanoic acid (3.95 g, 15 mmol) was added slowly dropwise with stirring a solution of sodium hydroxide (1.0 g, 25 mmol) in 7.0 mL of water. Stirring was continued for an additional 10 min. Then the reaction mixture was heated at 70 °C. This gave a residue to which 50 mL of water was added, and the resulting mixture was filtered. Acidification of the alkaline filtrate gave **8d** as a white solid. Recrystallization of crude product using hexane/methanol mixture gave colorless crystals (3.51 g, 84%): mp 75−77 °C (lit.[11g] mp 77−78 °C); TLC ($CHCl_3$, R_f 0.5); ^1H NMR ($CDCl_3$, 90 MHz) δ 1.25−1.80 (s + "br" m, 16H), 2.40 (t, 2H), 3.95 (t, 2H), 6.85−7.00 (m, 3H), 7.20−7.40 (m, 2H); IR (Nujol) 1690, 1235 cm^{-1}; LRMS, EI, *m/z* (%) 278 (8).

General Procedure for the Synthesis of Ion-Paired Amphiphiles (1−4). The ion-paired amphiphiles (**1**−**4**) were synthesized by passage of a methanolic solution of freshly recrystallized CTAB (1 equiv) through a column (9 cm × 1.5 cm) filled with freshly washed ion-exchange resin (Amberlite IRA-900, OH^- form). The eluents were collected together, and to this were added 0.5 equiv of **8a**, **8b**, and **8c** for **1**−**3** or 1 equiv of **8d** for **4**, respectively. Upon completion of this step the respective mixture was stirred at room temperature for 24 h under a nitrogen inlet. Then the solvent was evaporated under vacuum, and the solid obtained was recrystallized several times from a mixture of MeOH:EtOAc (1:10). This procedure afforded yields of ∼90−95% for all the ion-paired systems, **1**−**4**. IR confirmed the absence of a carboxylic acid moiety and the appearance of the ammonium carboxylate ($Me_3N^+\cdots{}^-O_2C$) group (∼1560 cm^{-1}).

All compounds (**1**−**4**) were found to be quite hygroscopic, and all of them crystallized as hydrates despite prolonged drying under vacuum. IR and repetitive elemental analyses confirmed the presence of water molecules in them. High resolution ^1H NMR spectra of **1**−**4** also confirmed the presence of an additional peak possibly due to hydration. However, this additional peak could be vanished upon treatment with D_2O as they were found to be fully exchangeable with D_2O. All the compounds gave satisfactory ^1H NMR, IR, and C,H,N analysis. Pertinent spectroscopic (^1H NMR, IR) and analytical (elemental analyses) data are given below.

Bis(hexadecyltrimethylammonium)phenyl-1,2-di(oxyundecanoate) (1): mp 110−130 °C; ^1H NMR (200 MHz, $CDCl_3$) δ 0.88 (t, 6H), 1.25−1.76 (s + "br" m, 88H), 2.16 (t, 4H), 3.06 ("br" m, exchangeable with D_2O), 3.32−3.40 (sharp s + m, 22H), 3.98 (t, 4H), 6.88 (s, 4H); IR (Nujol) 1560 cm^{-1}. Anal. Calcd for $C_{66}H_{128}N_2O_6$, H_2O: C, 74.52; H, 12.32; N, 2.63. Found: C, 74.49; H, 12.21; N, 2.38.

Bis(hexadecyltrimethylammonium)phenyl-1,3-di(oxyundecanoate) (2): mp 50 °C; ^1H NMR (200 MHz, $CDCl_3$) δ 0.88 (t, 6H), 1.25−1.75 (s + "br" m, 88H), 2.17 (t, 4H), 2.34 (s, exchangeable with D_2O), 3.36−3.44 (sharp s + m, 22H), 3.93 (t, 4H), 6.45−6.50 (m, 3H), 7.14 (apparent t, 1H); IR (Nujol) 1560 cm^{-1}. Anal. Calcd for $C_{66}H_{128}N_2O_6$, H_2O: C, 74.52; H, 12.32; N, 2.63. Found: C, 74.45; H, 12.28; N, 2.43.

Bis(hexadecyltrimethylammonium)phenyl-1,4-di(oxyundecanoate) (3): mp 105−110 °C; ^1H NMR (270 MHz, $CDCl_3$) δ 0.88 (t, 6H), 1.15−1.80 (s + "br" m, 88H), 2.1 ("br" s, exchangeable with D_2O), 2.27 (t, 4H), 3.34−3.50 (s + m, 22H), 3.92 (t, 4H), 6.82 (s, 4H); IR (Nujol) 1550 cm^{-1}. Anal. Calcd for $C_{66}H_{128}N_2O_6$, H_2O: C, 74.52; H, 12.32; N, 2.63. Found: C, 74.41; H, 12.26; N, 2.41.

Hexadecyltrimethylammonium phenoxyundecanoate (4): mp 35 °C (soften), 80 °C (clear melt); ^1H NMR (200 MHz, $CDCl_3$) δ 0.88 (t, 3H), 1.16−1.77 (s + "br" m, 44H), 2.19 (s, exchangeable with D_2O), 2.24 (t, 2H), 3.40−3.49 (sharp s + m, 11H), 3.94 (t, 2H), 6.87−6.92 (m, 2H), 7.23−7.30 (m, 3H); IR (Nujol) 1560 cm^{-1}. Anal. Calcd for $C_{36}H_{67}NO_3$, 0.5 H_2O: C, 75.74; H, 12.00; N, 2.45. Found: C, 75.61; H, 11.81; N, 2.27.

Vesicle Preparation. Reverse-phase evaporation[24] method was applied for the preparation of vesicles from these ion-paired amphiphiles for transmission electron microscopy. Typically, 2.5 × 10^{-3} M vesicular suspensions in pure, deionized water were prepared in the presence of a 0.5% uranyl acetate solution. For microcalorimetric studies, fluorescence anisotropy measurements, UV−vis spectroscopy studies, and X-ray diffraction experiments, the required amount of the ion-paired surfactants was placed in a container and the solid dissolved completely in chloroform. The solvent was evaporated by keeping it continuously in high vacuum for 12 h to produce a film of the surfactant. This was then hydrated with deionized water, and the hydrated films were subjected to 4−5 freeze−thaw (above the phase transition temperature) cycles. The resulting opalescent solution was then sonicated to give stable aggregates. For entrapment experiments, the bath-sonicated vesicles were used. In all the cases, clear and optically translucent dispersions were obtained.

Transmission Electron Microscopy Studies. In all the cases, 2.5 × 10^{-3} M vesicular suspensions in deionized water were prepared in the presence of 0.5% (w/v) uranyl acetate solution by the reverse-phase evaporation method. Opalescent to optically clear aqueous dispersions were obtained in all the cases. One drop of the above dispersion was placed into a carbon−Formvar coated copper grid (400 mesh). Filter paper was employed to wick away excess water. It was then placed under a mechanical vacuum for approximately 0.5 h. A JEOL-TEM 200 CX electron microscope with an accelerating voltage of 120 keV was used for micrograph recording at magnifications of 57 000 and 96 000.

Light Scattering Experiments. Mean hydrodynamic diameters were determined by laser light scattering using Zetasizer 3000 (Malvern Instrument Ltd., Malvern, U.K). Light scattering employed a He−Ne laser source at a wavelength of 633 nm keeping the detector angle at 90°. Each suspension was generated by reverse-phase evaporation as described previously. The data were analyzed using internal instrument software involving Malvern 7132 digital (16-bit) autocorrelator. A 220 nm latex standard was used for calibration.

Entrapment of Riboflavin and Gel Filtration. The vesicles were prepared by bath sonication of the lipids (1 mg/1 mL) in aqueous riboflavin solution (concentration 2 × 10^{-5} M, pH 6.8) for 30 min at ∼60 °C. Since the lamellar phases formed from the ion-paired amphiphiles are extremely sensitive to the presence of salt, the trapping experiments were performed in pure water. After cooling to room temperature, the vesicle suspension (3 mL) was loaded onto a sephadex G-50 M (Pharmacia) column (26 cm × 1 cm) and eluted with water (pH 6.8). Fractions containing most of the vesicles were pooled. These contained riboflavin molecules that were bound to the vesicles at the outer surfaces and also the ones that got entrapped in the vesicular inner pools.

Kinetics of Transmembrane Permeation. An aliquot of 1 mL (pH 6.8) was taken in a fluorescence cuvette, and the time-dependent decrease in the fluorescence intensity at 514 nm (excitation at 374 nm, excitation and emission slit widths 10 and 20 nm respectively) with time at 25 ± 0.5 °C was followed using a Hitachi Model F-4500 fluorescence spectrophotometer upon adjustment of pH from 6.8 to 10.2 by the addition of an aliquot of 66.3 μL of a 0.034 M KOH solution. Since riboflavin fluorescence decreases upon ionization alkaline media (pK_a ∼ 10.2), the time-dependent loss of the fluorescence intensity at 514 nm due to riboflavin under an imposed transmembrane pH gradient of 3.4 pH units was taken as a measure of OH^- permeation across these vesicles. Rate constants were obtained from the monoexponential time dependent portion of the loss of the fluorescence intensity.

Differential Scanning Calorimetry. (a) Preparation of Surfactant Suspension for Calorimetry. Individual lipid dispersions in pure water (Millipore) were prepared by weighing an appropriate amount of the solid ion-paired surfactant into the DSC pan and adding 12 μL water. The pan was immediately sealed, transferred to the calorimeter, and kept at 80−90 °C to accomplish proper hydration. A 120 mmol solution of each compound was used for DSC measurements.

(b) Calorimetric Measurements. DSC measurements were carried out with a Perkin-Elmer Model DSC-2C differential scanning calorimeter at a sensitivity of 1 mcal/s and a scanning rate of 5 K/min. A pan containing an identical volume of pure water (Millipore) was used as reference in all cases. Heating and cooling thermograms for each sample were repeated several times to get reproducible thermograms. The peak in the excess heat capacity vs temperature plot was taken as the main transition temperature T_m. At different scanning rates, identical values of enthalpy, transition temperature, half-height width, and height of the transition profile were obtained. The transition enthalpy, ΔH, was determined by measuring the area under the transition profile and was the average of at least three separate isolated runs. This integral was used to calculate both the calorimetric (ΔH_{cal}) and van't Hoff (ΔH_{vH}) enthalpies of the transition. These enthalpies were used to determine the "cooperative unit" (CU) of the transition, the number of monomers undergoing the phase transition from the relationship CU = $\Delta H_{vH}/\Delta H_{cal}$. All the

thermodynamic parameters are the averages of at least two independent sample preparations, and each of the specimens was scanned at least three times. Main phase transition entropy, ΔS, in the units of cal mol^{-1} K^{-1}, was determined on the basis of the assumption that at the phase transition temperature, the gel, and the liquid-crystal like phases were in equilibrium. ΔS was measured from the equation $\Delta S = \Delta H_{cal}/T_m$, where ΔH is expressed in cal mol^{-1} and T_m in Kelvin. Phase transition temperatures (T_m) are accurate up to ±0.5 °C and enthalpies up to ±1.0 kcal mol^{-1}. The van't Hoff enthalpy ΔH_{vH} was obtained from the relation $\Delta H_{vH} = 6.9\ T_m^2/\Delta T_{1/2}$ where $\Delta T_{1/2}$ is the width at the half-maximum excess specific heat and is accurate within ±10%.

Microcalorimetry. Lipid vesicles (2.5 mmol) were made by the hydration of the dry lipid film. These hydrated films were subjected to 4−5 freeze−thaw (above the phase transition temperature) cycles and vortexed. Then individual samples were degassed under vacuum prior to the transfer to the sample cell. Identical volumes of vesicular suspension (1.2 mL) and water were loaded into the sample and reference cell, respectively, of an MC-2 ultrasensitive scanning calorimeter (Microcal Co., Amherst, MA). Samples were maintained for at least an hour below the gel-to-liquid-crystalline phase transition temperature before being scanned. The scan rate was 90 °C/h. The calorimeter was calibrated electronically. The transition enthalpy and van't Hoff enthalpy were obtained from the data analysis software (origin) coupled with it.

Fluorescence Anisotropy Studies. Steady state fluorescence measurements were carried out in a Hitachi F-4500 fluorescence spectrophotometer equipped with polarizers. Temperature was regulated by a constant temperature water circulating bath (model Julabo F10) through the sample cell holder. The samples were allowed to equilibrate for 10 min prior to each run, and the temperature of the sample was measured immediately prior to each measurement. Keeping the excitation wavelength fixed at 360 nm, the emission spectra in the wavelength region of 390−480 nm were studied using a band-pass of 5 nm. The fluorescence anisotropies (r) of DPH (8.6×10^{-8} M), as sensed by this probe doped in individual vesicular solutions (2.5 mM), were measured. At each temperature, the fluorescence emission spectra were recorded by adjusting the polarizers in four different positions. The anisotropy (r) at different temperatures for each vesicular solution was calculated by employing Perrin's equation, $r = (I_{II} - I_{\perp}G)/(I_{II} + 2I_{\perp}G)$ where, I_{II} and $I_{\perp}$ are the observed intensities measured with polarizers parallel and perpendicular to the vertically polarized exciting beam, respectively. G is a factor used to correct for the inability of the instrument to transmit differently polarized light equally. For each aggregate, an r vs T plot gave the information about the gel to liquid-crystalline phase change as function of temperature. The values reported herein for r are the average values of three independent measurements. The gel to liquid-crystalline phase transition temperatures were calculated from the midpoints of the breaks related to the temperature-dependent anisotropy values. The temperature range for the phase transition was calculated from the two temperature points for each experiment which marked the beginning and the end of the phase transition process.

UV−Absorbance Method. In a typical experiment, a mixture of BAA (2×10^{-5} M) and the ion-pair lipid (1×10^{-3} M) was first dissolved in 100 μL of ethanol and then from this ethanol was removed by keeping the sample in high vacuum for 12 h to produce a BAA-doped lipid film. Then 2.5 mL of water was added to this film, and the resulting mixture was first vortexed and then subjected to 4−5 freeze−thaw cycles. This gave a translucent BAA-doped vesicular solution. Then an aliquot of this sample was transferred into the sample cuvette, and to the reference compartment another vesicular sample of identical lipid concentration that did not contain any BAA was taken. The temperature of the cuvette chamber was maintained by a thermoelectric temperature controller, TCC-60. After attainment of a particular temperature, UV−vis spectra were recorded in a Shimadzu model UV 2100 spectrophotometer at various temperatures from 6 °C onward in the wavelength range of 200−450 nm. Similarly, during the cooling of the vesicular solutions, the spectra at different temperatures were also recorded. The plots of the ratios of the absorbances due to enol (315 nm) and to keto (250 nm), $[A_{enol}/A_{keto}]$, vs temperature (T) gave apparent T_m values for the individual vesicles.

Micropolarity and Phase Transition Temperature by Pyrene. A solution of pyrene in MeOH was introduced into a solution of a given ion-pair in $CHCl_3$. The solvent from this mixture was removed under vacuum. Water was added to the dry lipid film containing pyrene, and vesicles were obtained by freeze−thaw method. The vesicle and pyrene concentrations were 5×10^{-4} and 7.9×10^{-8} M, respectively. A Hitachi 650-60 spectrofluorimeter was used to determine the systemic micropolarities at various temperatures and apparent phase transition temperature (T_m). The temperature of the sample cell holder was regulated by circulating water using a constant temperature water bath (model Julabo F10). Keeping the excitation wavelength fixed at 337 nm, the emission spectra of the region 360−400 nm were recorded using bandwidths of 5 nm. The samples were allowed to thermally equilibrate for 10 min prior to each measurement. At each temperature, the ratio I_3/I_1, where I_3 and I_1 represent the intensities of the third and the first vibronic peaks in the fluorescence emission spectrum due to pyrene was recorded and plotted against T, the temperature. The measurements were done in the temperature range of 25−70 °C. The value of I_1/I_3 also gives an idea about the micropolarity of the vesicular suspension.

UV−Visible Spectroscopy. A 2.5 mmol vesicular suspension was prepared as described previously. UV−vis spectra of ion-paired systems **1**, **2**, **3**, and **4** were taken separately as solutions in pure $CHCl_3$ and in the form of vesicular aggregates in aqueous media at 25 °C using Shimadzu model 2100 UV−visible recording spectrophotometer. Spectra in the wavelength range of 190−500 nm were recorded.

X-ray Diffraction Studies. Self-supported cast films for the X-ray diffraction studies were prepared by dispersing the amphiphile in water (10 mg/1.0 mL) as described above. Few drops of this suspension at hot condition were dispersed on a precleared glass plate and air-dried at room temperature. Finally it was kept under vacuum for 15 min. X-ray diffraction was carried out by the reflection method with a X-ray diffractometer (model XDS-2000 Scintag Inc., USA). The X-ray beam was generated with a Cu anode and the wavelength of $K\alpha_1$ beam was 1.5406 Å. The X-ray beam was directed toward the film edge, and the scanning was done up to the 2θ value of 20°.

Molecular Modeling Studies. All five ion-paired amphiphiles were drawn, and their energy-minimized, preferred conformations were calculated using the INSIGHT II 2.3.5. package (DISCOVER, Biosym. Technologies). DISCOVER is a molecular simulation program that performs energy minimization to optimize initial geometries of different amphiphilic molecules constructed from appropriate fragments in INSIGHT. Minimization path followed conjugate gradient optimization. Consistent valence force field was selected for computations. Calculated thickness and preferred drawings of different amphiphilic monomers appear in Supporting Information.

Acknowledgment. This work was supported by a TDM grant of Genetic Engineering and Biotechnology and in part by a grant from HLRC, Bangalore. We are grateful to Professor A. Surolia for giving access to microcalorimeter, Dr. G. Subanna for TEM studies, and SERC for the computational facilities.

Supporting Information Available: ^{1}H NMR of **1**, **2**, **3** and **4**, mass spectra of **7a**, **7b**, and **7c**, and energy-minimized drawings of different ion-paired systems **1**−**4** (Figure 1, supplementary information) (14 pages). This material is contained in libraries on microfiche, immediately follows this article in the microfilm version of the journal, and can be ordered from the ACS; see any current masthead page for ordering information.

JO980315L